Chemical and Process Engineering: New Frontiers, 2025, 46(4), e112
DOI: 10.24425/cpe.2025.155550

Impact of freeze-drying parameters on the physicochemical properties of bacterial cellulose

Michał Kapała, Tobiasz Gabryś*

University of Bielsko-Biala, Faculty of Materials, Civil and Environmental Engineering, Institute of Engineering Sciences, Willowa 2, 43-309 Bielsko-Biala, Poland

Abstract
Nowadays, increasing attention is being given to the development of new applications for biopolymers such as bacterial cellulose (BC). The aim of this study was to evaluate the influence of freeze-drying conditions on the physicochemical properties of bacterial cellulose, which may, in the future, support the advancement of biomedicine and broaden the applicability of natural materials. Freeze-drying (FD) was chosen due to its ability to preserve the internal structure of the material to a much greater extent than conventional drying. Furthermore, it allows for long-term storage of samples, which facilitates distribution. Bacterial cellulose samples were analyzed. Their mass, diameter, and thickness were measured before and after either freeze-drying and conventional drying, allowing for the assessment of shrinkage and secondary water absorption. Additionally, freeze-dried samples were examined using scanning electron microscopy (SEM) to analyze their porosity. The results showed that conventional drying disqualifies bacterial cellulose as a viable material for industrial applications. In contrast, freeze-dried samples, despite variations in shrinkage, porosity, and water absorption, retained high similarity to their original structure, making them more promising for future use in biomedical and biotechnological applications. In addition, through digital microscopic image analysis, the significant effect of conditions; including freeze-drying temperature on the internal structure of the material under study was demonstrated.

* **Corresponding author, e-mail:**
tgabrys@ubb.edu.pl

Article info:
Received: 21 July 2025
Revised: 17 September 2025
Accepted: 15 October 2025

Keywords
bacterial cellulose, freeze-drying, biopolymers processing, SEM, computer modelling

1. INTRODUCTION

Cellulose is one of the most widespread natural polymers on earth (Wertz et al., 2010). It has been known and used for centuries, especially cellulose of plant origin, both in native and processed forms (Jing et al., 2024). A very interesting type of cellulose that, apart from its chemical structure, has nothing to do with plants is bacterial cellulose (BC). Bacterial cellulose is a polysaccharide produced by certain species of bacteria, mainly of the genus *Komagataeibacter* (Iguchi et al., 2000). It is an alternative to traditional plant cellulose, offering a number of unique properties due to its high chemical purity, lack of lignin and hemicelluloses (Esa et al., 2014), highly organized nanofiber structure (Chen et al., 2022), large specific surface area and high degree of crystallinity (Almeida et al., 2022; Castro et al., 2011). Thanks to these characteristics, bacterial cellulose exhibits excellent absorbency (Luo et al. 2019), flexibility (Prilepskii et al., 2023), mechanical strength and biocompatibility, making it an attractive material for biomedical engineering applications, particularly as a dressing material, drug carrier or cell culture matrix (Choi et al., 2022; Joseph et al., 2025). One of the key aspects of preparing bacterial cellulose for biomedical applications is its proper fixation and preservation. Due to its naturally high water content, even above 90%, it is essential to use a drying process that allows for its long-term storage and further use. However, traditional drying methods, such as convection, heat, vacuum or ethanol drying, often lead to significant structural changes in the material, such as volumetric shrinkage, reduced porosity or a decrease in absorbent capacity (Sozcu et al., 2024). These changes can significantly limit the functionality of bacterial cellulose in medical applications (Almeida et al., 2022). An alternative and increasingly widely used method of drying biomaterials is freeze drying, or sublimation drying, which involves removing water from frozen material under reduced pressure (Chen et al., 2020). This process, with appropriately selected parameters, allows to preserve the spatial structure of the material, minimizing the risk of deformation and degradation. The maintenance of porosity and the ability to reabsorb water is crucial from the point of view of dressing applications – as it determines the ability of the material to absorb wound exudate and maintain an appropriate level of moisture and gas exchange, which promotes tissue regeneration processes (Cherng et al., 2021). In addition, thanks to digital analysis of microscopic images, a significant effect of conditions; including freeze-drying temperature on the internal structure of the tested material was demonstrated. There are many reports in the literature on the use of bacterial cellulose in next-generation dressings (Pasaribu et al., 2023). However, there is a lack of conclusive data on the effect of specific freeze-drying conditions on the preservation of key structural and performance characteristics

of this material (Sozcu et al., 2024). Optimization of the drying process is of particular importance for preserving properties that determine the effectiveness of the dressing, such as secondary absorbency, fluid transport capacity, elasticity or surface bioactivity (Chen et al., 2022).

The aim of the present study was to determine the effect of freeze-drying conditions on selected physicochemical properties of bacterial cellulose, such as water absorption, secondary water absorption, volume shrinkage after drying, porosity, dimensional changes and internal structure analysed by optical and electron microscopy. The authors aspiration was to determine such process parameters that would maximize the preservation of the original, untreated internal structure of cellulose, guaranteeing optimal functional properties from the point of view of biomedical engineering. Optimization of the lyophilisation process can significantly influence the development of modern dressing materials based on natural biopolymers, in line with current trends in biomedicine, regenerative medicine and sustainable development of medical technologies.

2. EXPERIMENTAL WORK

2.1. Materials

The chemicals used for the preparation of the culture medium and for the purification of the obtained BC included: D-glucose ($\geq$ 99%), peptone from enzymatic digest of meat, and sodium hydroxide ($\geq$ 97%, pellets), all purchased from Sigma Aldrich (Darmstadt, Germany); yeast extract and micro agar purchased from Duchefa Biochemie (Haarlem, The Netherlands); disodium hydrogen phosphate dihydrate purchased from Merck (Darmstadt, Germany); citric acid purchased from Chempur (Piekary Śląskie, Poland); and acetic acid (99.8%) and ethanol (96%) purchased from Honeywell (Charlotte, NC, USA).

2.2. Microorganisms

The bacteria strains used in this study were *Komagataeibacter Intermedius* (LMG 18909) purchased from Belgian Coordinated Collections of Microorganism, which were maintained and precultured in the laboratory of Faculty of Materials, Civil and Environmental Engineering, University of Bielsko-Biala.

2.3. Preparation of samples

The reinforced acetic ethanol culture medium (RAE) used for bacterial cellulose production was selected for the biosynthesis process. The liquid medium contained glucose (40 g/L), peptone from meat (10 g/L), yeast extract (10 g/L), disodium hydrogen phosphate dihydrate ($Na_2HPO_4 \cdot 2H_2O$, 3.38 g/L), citric acid (1.37 g/L), acetic acid (10 mL/L), and ethanol (10 mL/L). The solid medium, used for bacterial revitalization and inoculation, included the same components with the addition of agar (10 g/L). All media were sterilized by autoclaving at 121 °C for 15 minutes, with the glucose solution autoclaved separately. Acetic acid and ethanol were added to the medium after autoclaving. The bioprocesses were carried out in 250 mL Erlenmeyer flasks equipped with membrane screw caps. Each flask, containing 50 mL of RAE medium, was inoculated with a single bacterial colony and incubated in a water bath for 7 days at 30 °C. During the first 24 hours, the flasks were shaken; after this period, shaking was stopped and the bioprocess was continued under static conditions. In this manner, bacterial cellulose samples were obtained. The prepared BC samples were subsequently washed with distilled water. Next, the purification process, which allows the removal of bacterial cell residues, was initiated using 0.5 M NaOH. The purification was carried out in a water bath at 80 °C for 1 hour with shaking. Then, they were washed again with distilled water up to neutral pH. The samples before and after neutralization are showed in Figure 1.

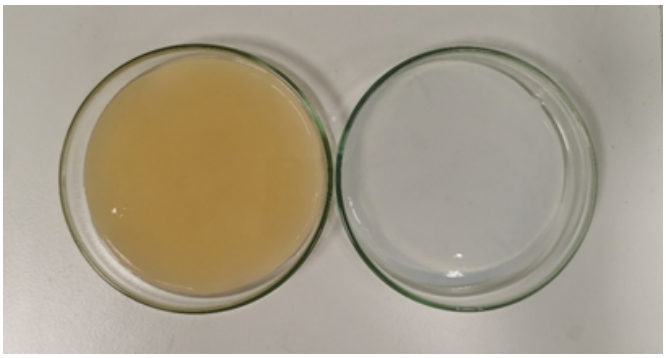

Figure 1. BC samples before (on the left) and after (on the right) neutralization.

2.4. Methods of drying

The goal of the work was to optimize the drying process to preserve the original structure of BC, so the process was carried out as follows. The reference sample was subjected to standard drying method (convective drying). The sample was placed in a laboratory dryer Binder model FD 115 (Tuttlingen, Germany) at a constant temperature of 40 °C in order to minimize the risk of structural damage and subjected to a drying process for 48 hours. This extended drying period ensured thorough dehydration of the material. After the drying cycle was completed, the sample was removed from the dryer and immediately transferred to an airtight container.

The remaining samples were freeze-dried under the following conditions. The freeze-drying process was carried out using a Kemolo HL-10 lyophilizer (Anhui, China). Three BC samples, underwent freeze-drying under different pre-freezing conditions. Each sample was first cooled to a specific temperature: –20 °C, –27.5 °C, and –35 °C, respectively, in order

to investigate the influence of freezing temperature on the final physicochemical properties of the material. Following the freezing stage, the samples were subjected to sublimation, during which they were gradually heated to 50 °C under reduced pressure (25 ∼ 35 Pa), allowing the removal of water in the form of vapour. After completion of the freeze-drying process, the dried samples were carefully transferred into tightly sealed containers to prevent exposure to moisture (Figure 2). The samples were stored in hermetically sealed containers under ambient conditions until further analyses and testing were performed. Table 1 shows the drying parameters along with the sample description system.

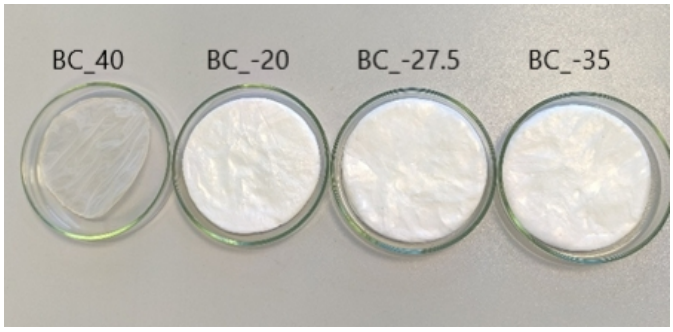

Figure 2. Comparison of the samples after convective and freeze-drying method.

2.5. Physicochemical properties

A digital caliper with an accuracy of 0.01 mm was used to measure the diameter and thickness of the samples before and after the drying process. These measurements allowed, in the next stages of the work, to determine properties such as volume and shrinkage after the drying process. Each sample was weighed both before and after the drying process using an analytical balance with an accuracy of 0.0001 g, which allowed for the determination of parameters such as water content. One of the research methods employed in this study was the rehydration of the dried BC samples. This process was designed to evaluate the material's ability to absorb water and return to its original hydrated form, which is particularly important in biomedical applications such as wound dressings or tissue engineering. The rehydration procedure was carried out by immersing the dried BC samples in distilled water and allowing them to soak at room temperature for a total duration of 24 hours. No agitation or external force was applied during the process. After the rehydration period, the samples were gently removed from the water and then analysed further to notice changes in their mass compared to original values with the post rehydration data made it possible to analyse the efficiency of rehydration water uptake in BC. The physicochemical study of all samples was repeated three times.

2.6. Microscopy analysis

The freeze-dried and convectively dried BC samples were subjected to analysis using scanning electron microscopy Phenom ProX (Thermo Fisher Scientific, Waltham, USA), which enabled detailed observation of the surface morphology and internal structure of the materials. Prior to analysis, the samples were sputtered with gold with a layer thickness of 15 nm in a low vacuum sputtering device Leica ACE-200 (Wetzlar, Germany). The obtained microphotographs were subjected to digital image processing with PoroMetric software with PIK Instruments to determine porosity.

3. RESULTS AND DISCUSSION

3.1. Physicochemical properties

The basic physicochemical properties regarding the water content of the material were determined first as the most important in the context of the material. The physicochemical properties of all obtained samples, such as: wet and dry mass and initial water content are shown in Table 2. The wet mass was measured immediately after synthesis for all samples using an analytical balance. As presented in Table 2, the values do not differ significantly from one another, showing a high level of consistency between samples. This similarity makes it easier to observe differences caused by the drying conditions. The dry mass was measured using the same balance after the drying process was completed and also showed a high similarity between the tested samples. Next, based on these data, the water content was calculated using the following Equation (1).

$$Wc = \frac{w - d}{w} \cdot 100 \quad (1)$$

where: Wc – water content [%]; w – weight in wet state [g]; d – weight in dry state [g].

Table 1. Drying parameters and sample description system.

Sample	Methods of drying	Drying time [h]	Initial temperature [°C]	Final temperature [°C]	Operating pressure
BC_40	convective drying	48	40	40	1010 hPa
BC_–20	freeze-drying	8	–20	50	25 ∼ 35 Pa
BC_–27.5		8.5	–27.5		
C_–35		9	–35		

Table 2. Physicochemical properties of obtained samples.

Sample	BC_40	BC_– 20	BC_– 27.5	BC_– 35
Weight in wet state [g]	23.2±0.4	23.5±0.3	23.1±0.3	23.0±0.4
Weight in dry state* [g]	0.1	0.1	0.1	0.1
Initial water content [g]	23.0±0.5	23.4±0.3	23.0±0.3	22.9±0.4
Initial water content [%]	99.5	99.5	99.5	99.5

*deviation = 0.003

The results clearly demonstrate the extremely high water content in BC, which amounts to approximately 99.5%. This indicates that BC is composed almost entirely of water, with the solid fraction representing only a minimal portion of its total mass (Rebelo et al., 2018). Such a high level of hydration reflects the material's highly porous, gel-like structure and its strong ability to retain water within its fibrous network (Takayama and Kondo, 2023). This characteristic is particularly relevant for biomedical and industrial applications, where moisture content and structural integrity are critical factors (Wahid et al., 2021). At the same time activities aimed at assessing the impact of the drying method on changes in the dimensions and volume of BC were also carried out. At this point, noticeable differences can be observed, depending on the drying method and conditions. They are shown in Table 3. These differences pertain to both the diameter and thickness of the samples, directly affecting the degree of shrinkage of the BC. The volume of the bacterial cellulose BC was calculated using the following Equation (2), while the shrinkage of the material results from the difference in the volume of the sample before and after the drying process – Equation (3).

$$V = \pi \cdot r^2 \cdot h \tag{2}$$

where: V – BC volume [cm^3]; r – radius of BC sample [cm]; h – thickness of BC sample [cm].

$$Sh = \frac{Vw - Vd}{Vw} \cdot 100\% \tag{3}$$

where: Sh – material shrinkage [%]; Vw – BC volume in wet state [cm^3]; Vd – BC volume in dry state [cm^3].

It is evident that the convectively dried sample differs significantly from its FD counterparts, showing a much lower ability to preserve its original structure, losing over 95% of its volume during the drying process (Du et al., 2025). Also during the study, a clear relationship was observed: lower freeze-drying temperatures resulted in reduced material shrinkage, indicating better preservation of the original structure of the tested samples; and consequently with the increase in rehydration (Figure 3). This relationship is due to the fact that smaller damage in the internal structure of the material, resulting in the collapse of pores, entanglement of cellulose nanofibers, occurs because the structure is more similar to the original. And this, in turn, translates into a larger area of physical water binding in the cellulose matrix and thus improved rehydration. Interestingly, our data indicate that freezing at lower temperatures (–27.5 °C and –35 °C) resulted in reduced volumetric shrinkage, in contrast to previous findings reported in the literature (Luo et al., 2020). This may suggest that, under our experimental conditions, smaller ice crystals and the resulting finer pore network provided enhanced mechanical stability during primary drying, limiting matrix collapse.

Rehydration of the examined samples was also performed, and the relationship between this process and the freezing temperature of each sample is presented in Figure 3. Based on the obtained results, it can be concluded that lower freezing temperatures promote better structural preservation. This is reflected in the reduced shrinkage of the sample (Table 3) and directly leads to a higher measured porosity (Table 4). As a result, each of the FD sample is capable of reabsorbing more than 63% of its original water mass. These findings suggest

Table 3. Dimensional parameters of BC.

Sample	BC_40	BC_–20	BC_–27.5	BC_–35
Average diameter in wet state [mm]	76.49 (±0.90)	77.28 (±1.63)	76.87 (±0.02)	77.74 (±0.02)
Average diameter in dry state [mm]	64.54 (±2.78)	74.58 (±1.17)	75.31 (±0.07)	76.43 (±0.79)
Average thickness in wet state [mm]	4.79 (±0.27)	4.79 (±0.58)	4.81 (±0.22)	4.78 (±0.85)
Average thickness in dry state [mm]	0.30 (±0.09)	4.37 (±0.89)	4.67 (±0.26)	4.71 (±1.29)
BC volume in wet state [cm^3]	22.01 (±1.31)	22.45 (±1.55)	22.32 (±0.61)	22.70 (±0.72)
BC volume in dry state [cm^3]	0.99 (±0.07)	19.09 (±1.29)	20.79 (±1.01)	21.62 (±0.87)
Material shrinkage after convectional/freeze drying [%]	95.5	15	6.9	4.7

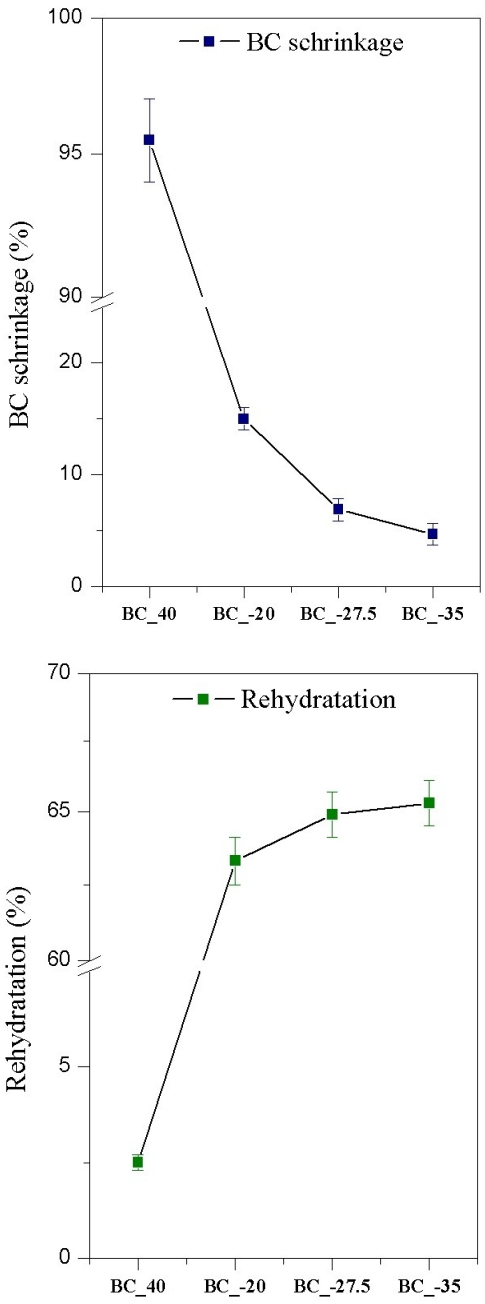

Figure 3. Influence of drying conditions on BC structural shrinkage and rehydration process.

Table 4. Results of pore indentification.

Sample	BC_40	BC_–20	BC_–27.5	BC_–35
Average pore area ratio [%]	0.51	46.72	63.17	63.98
Average circle equivalent diameter [nm]	516	285	487	417
Average major axis [nm]	748	376	649	570
Average minor axis [nm]	365	221	374	313
Average circumference [µm]	1.82	1.01	1.84	1.62

that BC FD may be an excellent technological solution for applications in the medical industry, considering its ability to regain properties very similar to those prior to the FD process.

3.2. Scanning electron microscopy

Below are the images of bacterial cellulose BC samples taken using a scanning electron microscope. Each image presents the surface of the dried or FD BC. These graphs allow for a detailed comparison of the structural differences resulting from the dehydration methods applied. The visible differences in pore size and distribution help assess how the drying technique influences the internal structure of BC (Fig. 4).

In the images presented above, important differences can be observed, particularly a higher degree of porosity in the FD samples. In contrast, in the case of the convectively dried sample, the fiber network collapsed, which also led to a reduction in the sample's volume. Similar observations were also reported by other authors (Sozcu et al., 2024; Vasconcellos and Farinas, 2018). The images of the FD samples also show visible differences in how densely the fibers are packed, which may be due to the different drying conditions used. These changes are likely to be reflected in the percentage of shrinkage in Fig. 3 for each sample. A higher level of fiber densification may suggest that the structure has partially collapsed, which could affect the material's properties (Pogorelova et al., 2024). This, in turn, determines the selection of optimal drying conditions that enable the industrial application of BC while maintaining adequate material properties and minimizing the time and costs associated with FD.

3.3. Pore properties

Porosity analysis was performed for each of the samples. This analysis was conducted due to the numerous physicochemical properties of BC that are directly related to its internal structure (Ul-Islam et al., 2013). Porosity analysis was performed based on digital processing of microscopic SEM images using an algorithm and tools to evaluate the surface area of the pores in relation to the surface area of the entire sample, thus determining the porosity of the material expressed as a percentage. Such a method is much faster and cheaper, as it allows to determine the porosity on the basis of SEM images, which are usually a mandatory part of the study anyway. The results of the analysis are shown in Fig. 5.

Based on the analysis of pore properties (Table 4) it was observed that the average pore area ratio of the BC_–20 sample differs by 16.45% compared to the BC_–27.5 sample, which is a significant difference, especially considering that difference between the BC_–27.5 and BC_–35 samples is only 0.81%. This result highlights how critical the decrease in freezing temperature from –20 °C to –27.5 °C is for maintaining the structure during the FD of BC samples. Important differences were also observed in the BC_–20 sample compared to the

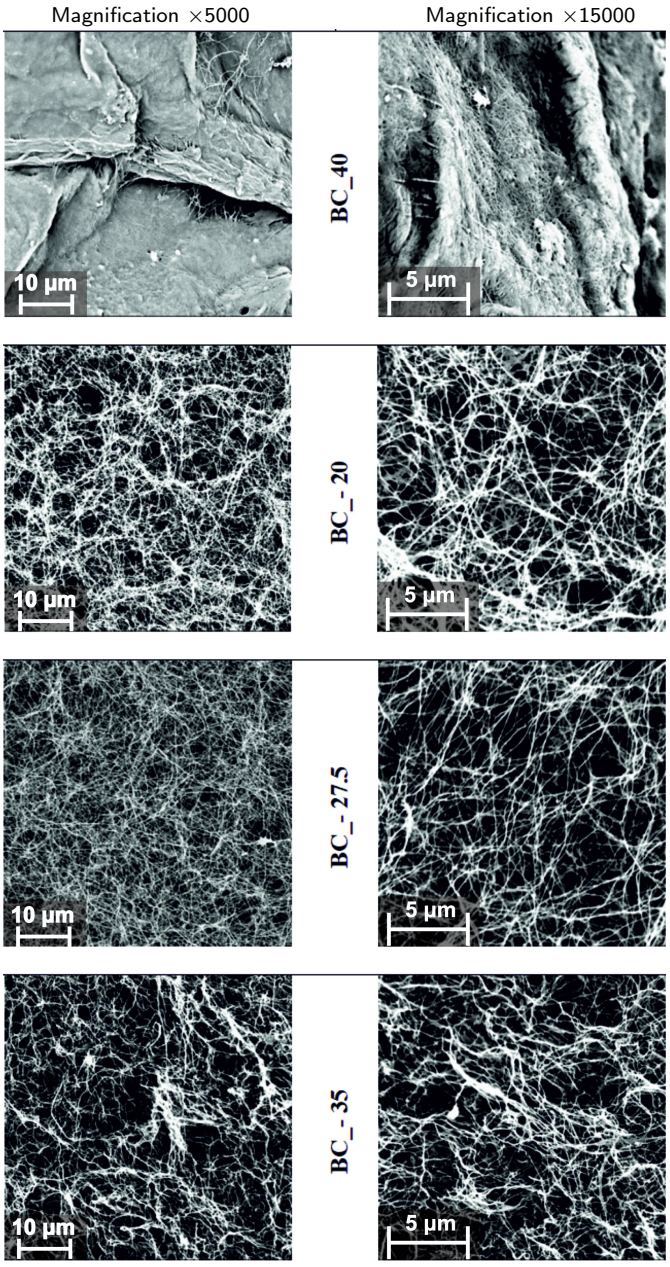

Figure 4. SEM images showing the obtained samples. Visible differences between convection-dried and freeze-dried samples.

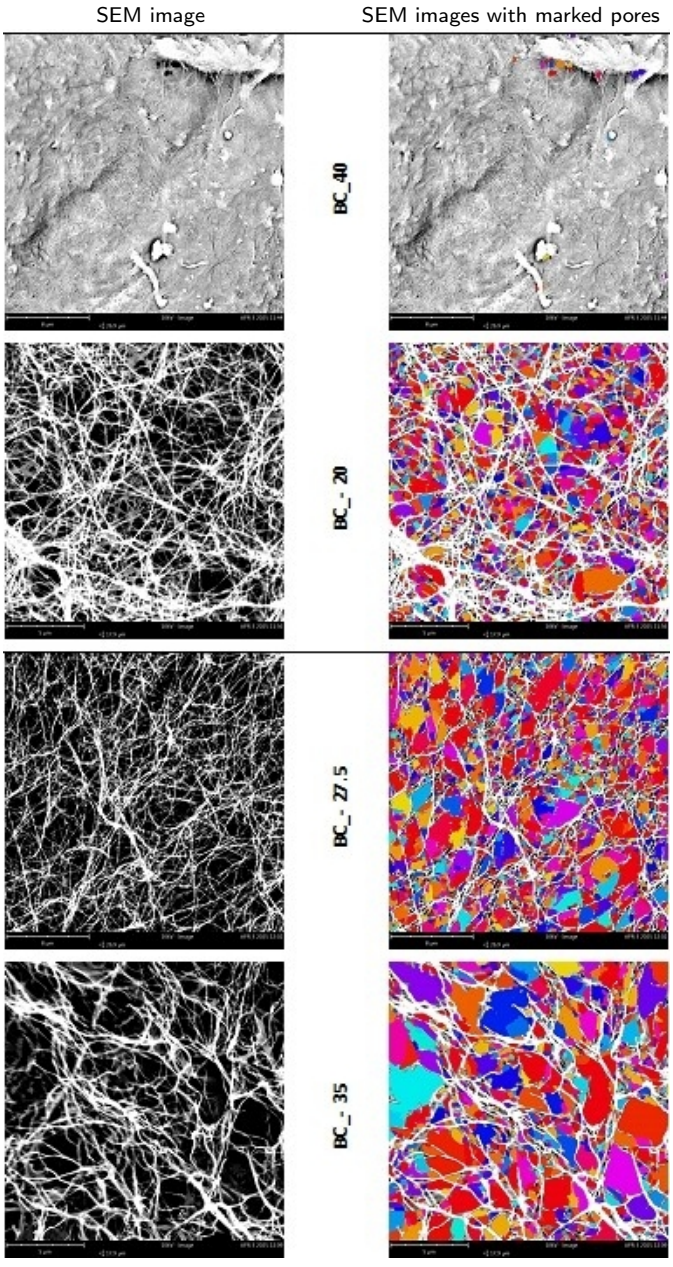

Figure 5. Comparison of SEM images before and after pore identification.

BC_–27.5 and BC_–35 samples regarding pore parameters such as average circle equivalent diameter, average major axis length, average minor axis length, and average circumference. It is suspected that these differences are directly correlated with the shrinkage of examined samples.

Furthermore the pore size distribution for each of the analysed samples is presented in Figure 6. They represent a typical Gaussian distribution, where the porosity is the sum or average of a very large number of small random factors, so that regardless of the distribution of each of these factors, its distribution will be close to normal. Based on analyses, conclusions can be drawn for each of the examined samples starting with sample BC_40, which did not allow the determination of the natural distribution of the pore size distribution due to its absence in the sample, which can also be seen in the SEM images and which is also confirmed by the work of other researchers (Illa et al., 2019). In the case of the BC_–20 sample, a greater variation in pore size was observed, ranging from 176 nm to 2.11 µm. However the vast majority of pores, approximately 95%, are within the range of up to 499 nm. This phenomenon is directly related to the previously mentioned 15% shrinkage of the sample (Table 3) as a result of which the originally larger pores were reduced in size. For the BC_–27.5 sample, it was observed that around 80% of the pores are within the range of up to 500 nm, indicating a smaller presence of

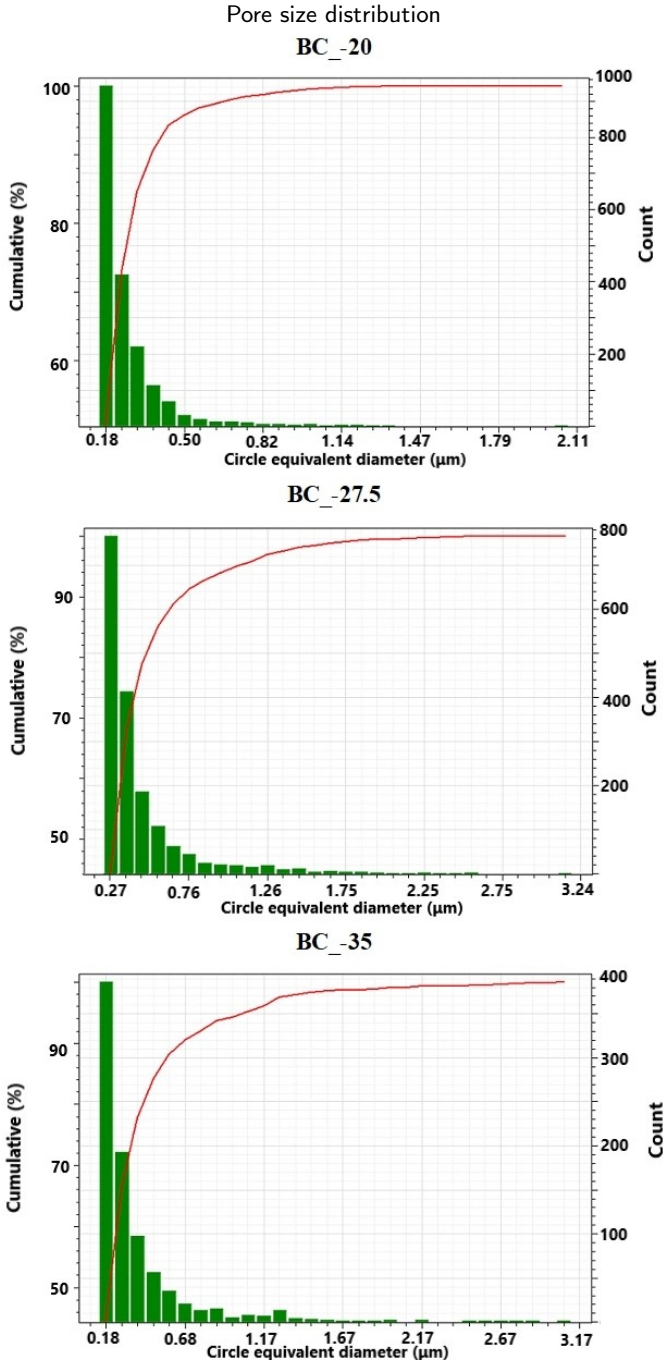

Figure 6. Pore distribution in BC samples.

small pores in the material's structure compared to BC_–20. Compared to samples dried at higher temperatures, the pore size distribution in this sample is noticeably broader with the largest pores reaching up to 3.24 µm. This suggests that lowering the freezing temperature to –27.5 °C allows for better preservation of the internal structure enabling the retention of larger pores. Such a pore size distribution may positively influence the sample's rehydration capacity and its ability to facilitate substance transport, which is particularly important for potential biomedical applications (Choi et al., 2022). For the BC_–35 sample, a pore size distribution similar to that of the BC_–27.5 sample was observed. However, BC_–35 contains a higher proportion of pores with diameters greater than 700 nm. The presence of a higher number of these larger pores has a direct impact on the total porosity of the sample, which is the highest among all the tested samples. This pore distribution suggests that lowering the freezing temperature to –35 °C further supports the preservation of the internal structure and minimizes sample shrinkage, allowing the development and retention of even larger pores. The obtained results suggest that lowering the freezing temperature during FD process may promote even better preservation of pores larger than 700 nm, which could consequently lead to a further increase in the overall porosity of BC.

4. CONCLUSIONS

Biopolymers may play a key role in the future as replacements for currently used solutions in medicine. In the case of biopolymers such as BC, one of the main challenges has been the issue of distribution, transportation, and storage, aiming to preserve their critical properties essential for medical applications. The most promising drying method, which allows the greatest similarity to the native sample to be maintained, proved to be FD. For comparison, one of the samples was dried using conventional convection drying. However, the results of this process completely disqualify it for potential biomedical use. Throughout the conducted research, a number of physicochemical properties of BC were evaluated in order to determine the optimal freeze-drying conditions suitable for industrial application. Based on the this research, the optimal freezing temperature was determined to be -27.5 °C, as it provides the best balance between preserving the original properties of bacterial cellulose BC and minimizing FD time. This is particularly important from the perspective of industrial production of medical products based on BC, where not only product quality but also process efficiency and scalability are critical.

ACKNOWLEDGMENTS

The authors are grateful to the University of Bielsko-Biala, for the financial support to cover the publications fee of this research article.

REFERENCES

Almeida A.P.C., Saraiva J.N., Cavaco G., Portela R.P., Leal C.R., Sobral R.G., Almeida P.L., 2022. Crosslinked bacterial cellulose hydrogels for biomedical applications. *Eur. Polym. J.*, 177, 111438. DOI: 10.1016/J.EURPOLYMJ.2022.111438.

Castro C., Zuluaga R., Putaux J.L., Caro G., Mondragon I., Gañán P., 2011. Structural characterization of bacterial cellulose produced by *Gluconacetobacter swingsii sp.* from Colombian agroindustrial wastes. *Carbohydr. Polym.*, 84, 96–102. DOI: 10.1016/J.CARBPOL.2010.10.072.

Chen C., Ding W., Zhang H., Zhang L., Huang Y., Fan M., Yang J., Sun D., 2022. Bacterial cellulose-based biomaterials: From fabrication to application. *Carbohydr. Polym.*, 278, 118995. DOI: 10.1016/J.CARBPOL.2021.118995.

Chen S.-Q., Cao X., Li Z., Zhu J., Li L., 2020. Effect of lyophilization on the bacterial cellulose produced by different *Komagataeibacter* strains to adsorb epicatechin. *Carbohydr. Polym.*, 246, 116632. DOI: 10.1016/J.CARBPOL.2020.116632.

Cherng J.-H., Chou S.-C., Chen C.-L., Wang Y.-W., Chang S.-J., Fan G.-Y., Leung F.-S., Meng E., 2021. Bacterial cellulose as a potential bio-scaffold for effective re-epithelialization therapy. *Pharmaceutics*, 13, 1592. DOI: 10.3390/pharmaceutics13101592.

Choi S.M., Kummara M.R., Zo S.M., Shin E.J., Han S.S., 2022. Bacterial cellulose and its applications. *Polymers*, 14, 1080. DOI: 10.3390/polym14061080.

Du M., Xiao Z., Luo Y., 2025. Sustainable strategies on cultivation, modification and rehydration of bacterial cellulose to overcome hornification for industrial applications: A review. *Carbohydr. Polym. Technol. Appl.*, 9, 100736. DOI: 10.1016/j.carpta.2025.100736.

Esa F., Tasirin S.M., Rahman N.A., 2014. Overview of bacterial cellulose production and application. *Agric. Agric. Sci. Procedia*, 2, 113–19. DOI: 10.1016/j.aaspro.2014.11.017.

Iguchi M., Yamanaka S., Budhiono A., 2000. Bacterial cellulose – a masterpiece of nature's arts. *J. Mater. Sci.*, 35, 261–270. DOI: 10.1023/A:1004775229149

Illa M.P., Sharma C.S., Khandelwal M., 2019. Tuning the physiochemical properties of bacterial cellulose: effect of drying conditions. *J. Mater. Sci.*, 54, 12024–12035. DOI: 10.1007/s10853-019-03737-9.

Jing L., Shi T., Chang Y., Meng X., He S., Xu H., Yang S., Liu J., 2024. Cellulose-based materials in environmental protection: A scientometric and visual analysis review. *Sci. Total Environ.*, 929, 172576. DOI: 10.1016/j.scitotenv.2024.172576.

Joseph A., Umamaheswari S., Vassou M.C., 2025. Bacterial cellulose: A versatile biomaterial for biomedical application. *Carbohydr. Res.*, 552, 109350. DOI: 10.1016/j.carres.2024.109350.

Luo C., Liu Z., Mi S., Li L., 2020. Quantitative investigation on the effects of ice crystal size on freeze-drying: The primary drying step. *Drying Technol.*, 40, 446–58. DOI: 10.1080/07373937.2020.1806865.

Luo M.-T., Huang C., Li H.-L., Guo H.-J., Chen X.-F., Xiong L., Chen X.-D., 2019. Bacterial cellulose based superabsorbent production: A promising example for high value-added utilization of clay and biology resources. *Carbohydr. Polym.*, 208, 421–430. DOI: 10.1016/j.carbpol.2018.12.084.

Pasaribu K.M., Ilyas S., Tamrin T., Radecka I., Swingler S., Gupta A., Stamboulis A.G., Gea S. 2023. Bioactive bacterial cellulose wound dressings for burns with collagen *in-situ* and chitosan *ex-situ* impregnation. *Int. J. Biol. Macromol.*, 230, 123118. DOI: 10.1016/j.ijbiomac.2022.123118.

Pogorelova N., Parshin D., Lipovka A., Besov A., Digel I., Larionov P., 2024. Structural and viscoelastic properties of bacterial cellulose composites: Implications for prosthetics. *Polymers*, 16, 3200. DOI: 10.3390/polym16223200.

Prilepskii A., Nikolaev V., Klaving A., 2023. Conductive bacterial cellulose: From drug delivery to flexible electronics. *Carbohydr. Polym.*, 313, 120850. DOI: 10.1016/j.carbpol.2023.120850.

Rebelo A.R., Archer A.J., Chen X., Liu C., Yang G., Liu Y., 2018. Dehydration of bacterial cellulose and the water content effects on its viscoelastic and electrochemical properties. *Sci. Technol. Adv. Mater.*, 19, 203–211. DOI: 10.1080/14686996.2018.1430981.

Sozcu S, Frajova J, Wiener J, Venkataraman M, Tomkova B, Militky J., 2024. Effect of drying methods on the thermal and mechanical behavior of bacterial cellulose aerogel. *Gels*, 10, 474. DOI: 10.3390/gels10070474.

Takayama G., Kondo T., 2023. Quantitative evaluation of fiber network structure–property relationships in bacterial cellulose hydrogels. *Carbohydr. Polym.*, 321, 121311. DOI: 10.1016/j.carbpol.2023.121311.

Ul-Islam M., Khattak W.A., Kang M., Kim S.M., Khan T., Park J.K., 2013. Effect of post-synthetic processing conditions on structural variations and applications of bacterial cellulose. *Cellulose*, 20, 253–263. DOI: 10.1007/s10570-012-9799-9.

Vasconcellos V.M., Farinas C.S., 2018. The effect of the drying process on the properties of bacterial cellulose films from *Gluconacetobacter Hansenii*. *Chem. Eng. Trans.*, 64, 145–150. DOI: 10.3303/CET1864025.

Wahid F., Huang L.-H., Zhao X.-Q., Li W.-C., Wang Y.- Y., Jia S.-R., Zhong C., 2021. Bacterial cellulose and its potential for biomedical applications. *Biotechnol. Adv.*, 53, 107856. DOI: 10.1016/j.biotechadv.2021.107856.

Wertz J.-L., Mercier J.P., Bédué O., 2010. Biosynthesis of cellulose, In: *Cellulose science and technology*. 1st edition, EPFL Press, New York, 46–80. DOI: 10.1201/b16496.